Transition from long- to short-lived transient pores in giant vesicles in an aqueous medium

Nicolas Rodriguez
CNRS, UMR 7099, Paris, F-75005 France
and Institut de Biologie Physico-Chimique, Laboratoire de Physico-Chimie Moléculaire des Membranes Biologiques, 13 rue Pierre et Marie Curie, Paris, F-75005 France

Sophie Cribier
CNRS, UMR 7099, Paris, F-75005 France;
Institut de Biologie Physico-Chimique, Laboratoire de Physico-Chimie Moléculaire des Membranes Biologiques, 13 rue Pierre et Marie Curie, Paris, F-75005 France
and Université Pierre et Marie Curie-Paris6, Paris, F-75005 France

Frédéric Pincet
École Normale Supérieure, Laboratoire de Physique Statistique, Paris, F-75005 France
and CNRS, UMR 8550, 24 rue Lhomond, Paris, F-75005 France

(Received 12 June 2006; revised manuscript received 24 August 2006; published 8 December 2006)

We have observed large pores in the membrane of giant vesicles in an aqueous medium. The lifetime of the pores can reach 2 min and their size (a few micrometers) enables their visualization by fluorescence microscopy. These pores are obtained thanks to a destabilization of the membrane due to the synergistic action of a cone-shaped and nitrobenzodiazole (NBD) labeled phospholipid illuminated in the presence of dithionite. The opening of the pore occurs immediately after illumination starts so that it can be accurately triggered. A concomitant decrease of the vesicle radius is observed; we interpret it as a solubilization of the membrane. Depending on the rate of this solubilization, long- or short-lived pores were observed. At the transition between both regimes for a 30 μm vesicle, the solubilization rate was about $1/300\ s^{-1}$. In order to interpret these observations, we have revisited the current model of pore opening to take into account this solubilization. This proposed model along with simulations enables us to prove that solubilization explains why the large long-lived pores are observed even in an aqueous medium. The model also predicts the solubilization rate at the transition between a single long-lived pore and a cascade of short-lived pores.

DOI: 10.1103/PhysRevE.74.061902 PACS number(s): 87.16.Dg

I. INTRODUCTION

Liposomes are widely used for many applications, including drug delivery. In that case, a drug encapsulated in a liposome must be directed and released in a controlled manner [1,2]. Drugs can be released from liposomes after endocytosis, by rupture of liposomes, or by slow permeation through their membrane [3,4]. In the latter cases, it is necessary to understand the parameters that drive the disruption of a membrane possibly interacting with proteins. Liposomes are also used as model systems to study biological membranes. A very important role is their use to study the behavior of membrane proteins. These proteins must be inserted in the liposome membrane first and protocols always employ solubilization of the native membrane by various detergents possibly followed by a reconstitution in liposomes when detergents are removed. The different steps of solubilization and liposome formation should however be better understood to improve these difficult reconstitutions [5–8]. It has already been shown with several detergents, that one of the early stages of the solubilization process involves porous liposomes [9,10]. This structure may be responsible for unwanted random orientation of reconstituted proteins in proteoliposomes [11]. Identification of the mechanisms responsible for pore formation in liposomes or cells is also very important for a better understanding of electroporation processes [12–14].

Recently, transient large pores have been observed in giant unilamellar vesicles under various conditions [15–17]. The system we present here is to our knowledge the only one that combines the following advantages: large transient pores are observed in an aqueous medium without proteins or a large excess of detergents and their opening can be precisely triggered. In order to obtain such pores in an aqueous medium, we have induced a solubilization of the membrane that forces the vesicle to constantly maintain a non-negligible surface tension. The rate of this solubilization turned out to be one of the main parameters that control the lifetime of the pore. Below a critical rate, only short-lived pores (less than 5 s) are observed. Long-lived pores appear only above this critical rate. Their long lifetime enables a quantitative study of the biophysical parameters that control the formation of the pores via an adaptation of a model previously developed [18]. This proposed model reveals that the transition between long- and short-lived pores is directly dependent upon the solubilization rate.

II. MATERIAL AND METHODS

A. Materials

Dioleoyl-*sn*-phosphatidylcholine (DOPC) is purchased from Sigma (Sigma-Aldrich, St Louis, USA). 1-egg-2-{6-[(7-nitro-2-1,3-benzoxadiazol-4-yl)amino]hexanoyl}-sn-glycero-

3-phosphocholine (C6-NBD-PC) and 1-egg-2-{12-[(7-nitro-2-1,3-benzoxadiazol-4-yl)amino]stearoyl}-sn-glycero-3-phosphocholine (C18,12-NBD-PC) are synthesized in our laboratory according to the protocol described elsewhere [19]. C6-NBD-PC are phospholipids with a six-carbon chain bearing a NBD at its end and C18,12-NBD-PC are phospholipids with an 18-carbon chain bearing a NBD on the 12th carbon. The sodium hydrosulfite (dithionite) is purchased from Sigma.

B. Giant unilamellar vesicle formation and observation

Giant unilamellar vesicles (GUV) made of pure DOPC are prepared by the electroformation method [20] as described in Ref. [21]. They are formed in a sucrose solution and observed in glucose solution. The concentrations (295 mM sucrose and 300 mM glucose) are set to allow a slight deflation due to osmotic pressure difference. The difference in molar mass of the two sugars induces sedimentation. The pressure difference between the inner and outer media of the GUV is zero so that the initial surface tension of the membrane is expected to be very small.

The vesicles are observed by epifluorescence and optical microscopy on an inverted microscope [Zeiss IM35 (Carl Zeiss, Oberkochen, Germany)] with ×25 immersion objective (Zeiss, NA 0.8). The fluorescence is excited by a Zeiss mercury lamp ($P=50$ W) with a blue-violet filter from Spindler & Hoyer (max. wavelength: 436 nm) (Linos photonics, Milford, USA). Images are acquired on a cooled 12-bit digital camera [Micromax, Roperscientific (Roper Industries, Duluth, USA)] and later analyzed using the Image J software (NIH).

III. RESULTS

A. Large transient pores in GUV: Principles and model

The formation and closing of pores in a vesicle result from a competition between two forces: surface tension and line tension. The membrane surface tension derives from the unfolding of membrane undulations and the stretching of the lipids. This force can rupture the membrane, leading to the formation and stabilization of open pores. On the other hand, at the rim of the pore, the lipids are forced to reorganize in order to reduce the interface between their hydrophobic part and the solvent. This reorganization leads to a line tension, which is always high for cylindrical shaped lipids. The line tension forces the pore to close up. The chronology of a pore life can be decomposed in three main stages. Firstly, the surface tension must increase to reach a rupture tension (possibly of the order of a few mN/m [22]). Secondly, the pore nucleates, likely on a defect of the membrane, inducing a rapid decrease of the surface tension. Thirdly, some of the inner solution flows out through the pore while the line tension closes it. This balance between the line and surface tensions will be critical in the duration of the second and third stages, i.e. the kinetics of opening and closing of the pore. Assuming the rupture tension is reached, it is possible to quantify more precisely these kinetics and it has already been described in detail elsewhere [18]. We will just summarize it briefly.

The kinetics of the pore radius, r_{pore}, is driven by the competition of the line tension, ζ, and surface tension, σ,

$$\frac{dr_{pore}}{dt} = \frac{r_{pore}(t)}{2\eta_{mb}}\left[\sigma(t) - \frac{\zeta}{r_{pore}(t)}\right], \tag{1}$$

where η_{mb} is the membrane viscosity.

The apparent radius of the vesicle, R_{ves}, decreases because inner medium is expelled through the pore. The origin of this leak is the pressure difference between the inside and outside media of the vesicle due to surface tension (osmolarity is the same in both media and thus does not play any role in the pressure difference). The leaking velocity, ν_{leak}, will therefore be critical for this decrease. It has been shown [18,23] that

$$\nu_{\mathrm{leak}} = \frac{\Delta P r_{\mathrm{pore}}}{3\pi\eta_{\mathrm{sol}}} = \frac{2\sigma r_{\mathrm{pore}}(t)}{3\pi R_{\mathrm{ves}}(t)\eta_{\mathrm{sol}}}, \tag{2}$$

where ΔP is the pressure difference between the inner and outer media, and η_{sol} the viscosity of the solution. The volume of the vesicle, V_{ves}, varies as

$$\frac{dV_{\mathrm{ves}}}{dt} = -\pi r_{\mathrm{pore}}^2 \nu_{\mathrm{leak}} = 4\pi R_{\mathrm{ves}}^2 \frac{dR_{\mathrm{ves}}}{dt}. \tag{3}$$

Equations (2) and (3) lead to

$$\frac{dR_{\mathrm{ves}}}{dt} = -\frac{r_{\mathrm{pore}}^3(t)\sigma(t)}{6\pi\eta_{sol}R_{\mathrm{ves}}^3(t)}. \tag{4}$$

With the reasonable assumption that ζ is constant, Eqs. (1) and (4) indicate that $\sigma(t)$, $R_{\mathrm{ves}}(t)$, and $r_{\mathrm{pore}}(t)$ are the three variables of the problem. Therefore, another equation is necessary. In Ref. [16], the authors chose to take a linear relation between the apparent area of the vesicle and the surface tension. We believe this assumption is often too drastic. We have chosen to use a more complicated but more precise equation that relates the difference between the real surface, A_r, and the projected surface, A_p, and σ [24],

$$\frac{A_r - A_p}{A_p} = \frac{k_B T}{8\pi k_c} \ln\left(\frac{\pi^2/a + \sigma/k_c}{\pi^2/A_p + \sigma/k_c}\right), \tag{5}$$

where k_b is the Boltzmann constant, k_c is the curvature modulus, and a is the area per lipid. A_r and A_p have now to be expressed as a function of R_{ves} and r_{pore}. When the pore is open,

$$A_p(t) = 4\pi R_{\mathrm{ves}}^2(t) - \pi r_{\mathrm{pore}}^2(t). \tag{6}$$

The real surface fluctuates around the projected surface. It is consequently larger than the projected surface area. It is given by

$$A_r = Na = Na_0(1 + \sigma/k_s). \tag{7}$$

$2N$ is the total number of lipids, which is commonly assumed to be constant during the lifetime of the pore. Taking into account a possibly variable number of lipids is an important improvement over the previous model that will be shown to be necessary to explain our experiments. a_0 is the

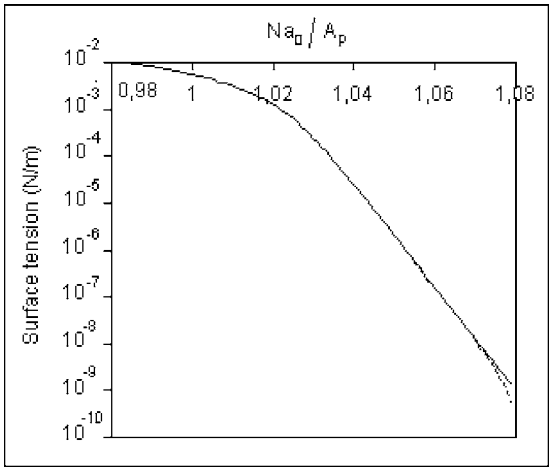

FIG. 1. Tension vs the ratio between the real area of the vesicle at zero tension, Na_0, and the apparent area of the vesicle, A_p, as deduced from Eq. (8). The parameters are given in Table I. The equation is drawn for $A_p=4\pi$ $(30\ \mu\text{m})^2$ (solid line) and $A_p=4\pi$ $(8\ \mu\text{m})^2$ (dotted line, distinct from the solid line only for $\sigma < 10^{-8}$ N/m). Tension is a function of N and A_p but depends only of N/A_p provided that $\sigma/k_{\text{courb}} \gg \pi^2/A_p$.

area per lipid at zero tension and k_s the stretching modulus.

The combination of Eqs. (5)–(7) provides the third equation for $R_{\text{ves}}(t)$, $r_{\text{pore}}(t)$, and $\sigma(t)$,

$$\frac{Na_0[1+\sigma(t)/k_S]}{4R_{\text{ves}}^2(t)-r_{\text{pore}}^2(t)}-1 = \frac{k_BT}{8k_c}\ln\left(\frac{\pi^2/a_0(1+\sigma/k_S)+\sigma/k_c}{\pi/[4R_{\text{ves}}^2(t)-r_{\text{pore}}^2(t)]+\sigma/k_c}\right). \quad (8)$$

This equation is rather awkward; we have numerically solved it. The result is shown on Fig. 1. For $\sigma > 10^{-8}$ N/m and $R_{\text{ves}} > 5$ μm (this will be shown to be true during all the pore opening and closing sequences considered in this article), Eq. (8) is very well approximated by

$$\frac{Na_0(1+\sigma/k_s)}{4R_{\text{ves}}^2(t)-r_{\text{pore}}^2(t)}-1=\frac{k_BT}{8k_c}\ln\left(\frac{\pi^2k_c}{a_0\sigma}\right). \quad (9)$$

Unfortunately, it still requires a numerical resolution. When 10^{-4} N/m $> \sigma > 10^{-8}$ N/m, an analytical expression of σ is correct,

$$\sigma=\frac{\pi^2k_c}{a_0}\exp\left[\frac{8\pi k_c(1-Na_0/A_p)}{k_BT}\right]. \quad (10)$$

This expression can be used during the slow closing of a pore but not during its opening, since σ should be close to the rupture tension (few mN/m [22]).

Without any simplification, pores dynamics are completely described by Eqs. (1), (4), and (8). Typical values of the various parameters are summarized in Table I.

B. The difficulty to obtain pores in aqueous medium

With a simplified Eq. (8), the model has already been used to describe experiments in which long-lived pores were observed [18] in a very viscous medium with a high concentration of glycerol (final viscosity 32 times that of water). The lifetime of the pore τ is typically given by [25],

$$\tau=\frac{3\pi\eta_{\text{sol}}R_{\text{ves}}^2}{2\zeta}. \quad (11)$$

In this viscous medium, these authors found a line tension of the order of 10 pN for DOPC vesicles.

Taking this value for ζ and typical values for R_{ves}, τ becomes of the order of 200 ms in an aqueous medium. To cross-check this result, we numerically solved Eqs. (1), (4), and (8) with MATHEMATICA (see a more detailed description of this approach below). The results show that the pore lifetime is less than 1 s. Because of their short lifetime, such pores would be difficult to directly observe.

TABLE I. Notation, values used in the numerical calculations and sources

	Notation	Value	Source
Membrane viscosity	η_{mb}	3.10^{-7} Nm^{-1} s	Ref. [25]
Solution viscosity	η_{sol}	1.3 cP	
Bending modulus	k_c	4.10^{-20} J	Ref. [30]
Stretching modulus	k_s	0.27 Nm^{-1}	Ref. [22]
Area per lipid	a_o	0.7 nm^2	Ref. [31]

C. Pores in aqueous medium

In aqueous medium, the viscosity cannot be varied; it remains of the order of 1 cP. For example, in the experiments we will present below, the viscosity of the inner medium η_{sol}, is 1.3 cP (295 mM sucrose solution). Thus, we had to adjust the remaining parameters in order to try to obtain long-lived pores. From Eq. (1), it is clear that ζ should be decreased while σ should constantly be kept as high as possible. We found a way to achieve these two goals simultaneously. When illuminated in the presence of dithionite, fluorescent C6-NBD-PC lipids induce a noticeable decrease on the size of the vesicles. This fact is seen in Fig. 2 where an example of the evolution of the vesicle radius is shown. Within about 5 min, the radius of the vesicles can be reduced by half and the vesicles often finally burst when a continuous illumination is maintained. Such a large reduction of the size of the vesicles can only be due to the loss of membrane lipids. Hereinafter, we will call this loss a "solubilization" of the membrane: The lipids may be solubilized in micelles or smaller vesicles, or damaged during the protocol. Photoinduced surface tension has already been used to open long-lived pores (illumination with a laser for several tens of minutes [25]). The mechanism by which the laser beam induced surface tension is unknown. It is likely that there was a modification of the surface area per molecule and/or extraction of part of the lipids in the membrane. A large loss of lipids due to intense laser illumination of a vesicle membrane has also been reported [26] without any microscopic model. A possible photo-oxidation of lipids that increases their solubility has been hypothesized [25]. The value of our approach

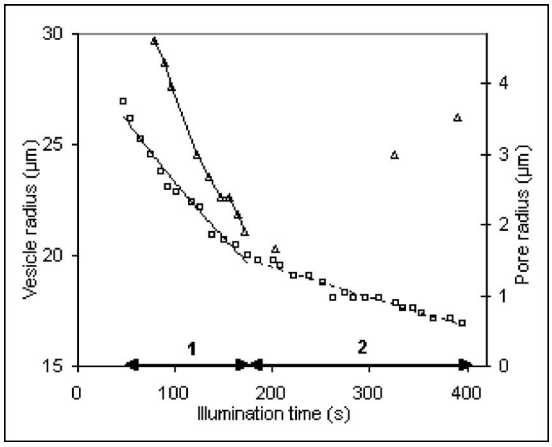

FIG. 2. Evolution of the radius of a vesicle under constant illumination. This radius decreases by 40% in 7 min, which corresponds to the loss of about 2/3 of the vesicle surface before its bursting. At first, the solubilization is quick (τ=215 s) and a pore is stabilized for 90 s (Stage 1). Then, the solubilization becomes slower (τ=715 s) and a cascade of short-living transient pores is observed (Stage 2). τ is obtained by the exponentially decreasing fits of the vesicle radius decay during each stage 1 (solid line for stage 1 and dotted line for stage 2). △: measured pore radius, symbols are linked when they correspond to a single pore that remains open. □: measured vesicle radius.

is the high speed of solubilization: It can be quick enough to be comparable with pore lifetime and thus play a role in maintaining the surface tension.

This solubilization decreases the number of lipids in the vesicle and therefore maintains σ significantly higher than it would be without solubilization [as can be seen from Eq. (8)]. Since C6-NBD-PC lipids also have a conical shape, they will gather at the rim of the pore and tend to reduce ζ. This reduction of ζ will be verified *a posteriori* from our experimental results. Therefore, vesicles with C6-NBD-PC lipids illuminated in presence of dithionite are good candidates to display pores in aqueous media.

In order to obtain this configuration, we have used the following protocol. A solution of C6-NBD-PC is injected near DOPC vesicles. The final concentration of C6-NBD-PC is 3 μM. These lipids spontaneously insert in the DOPC bilayer. The proportion of C6-NBD-PC reaches almost 10% in the vesicles in a few minutes [27]. This amount is estimated by comparison with vesicles made of a controlled amount of DOPC and C18,12-NBD-PC. The simple addition of C6-NBD-PC is sufficient to induce a destabilization that seems strong enough to favor a transbilayer movement of lipids and equilibration of C6-NBD-PC concentrations between outer and inner leaflet that may be attributed to small nanopores [27]. However, at this stage, no stretching of the vesicle is observed and there is no visible bilayer disruption. To induce surface tension, dithionite and illumination are required. Consequently, we add a drop of iso-osmotic dithionite solution near the vesicles so that the final dithionite concentration is 4 mM. The dithionite is added 30–45 min after the C6-NBD-PC when the fluorescence of the GUV reaches a plateau. Finally the cooperative action of C6-NBD-PC, dithionite and a few seconds of illumination with a mercury lamp

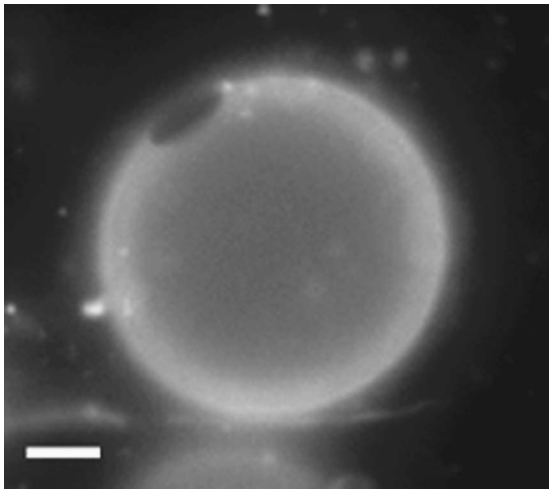

FIG. 3. Fluorescence microscopy image of a giant vesicle exhibiting a long-living transient pore. The bar represents 10 μm and the pore remained open for more than 80 s.

induce a fast stretching of the vesicles, probably due to the solubilization of the bilayer as mentioned previously. The subsequent increase of σ is sufficiently high to nucleate long-living large transient pores (Fig. 3). The nucleation spot may be a defect in the membrane, possibly one of the nanopores that have been hypothesized on these vesicles' surfaces [27]. The lifetime of the pores can reach several minutes in aqueous medium. Their sizes fall into a range of a few micrometers. In most experiments, pores are transient and the vesicle does not burst before its resealing (but a bursting occurs sometimes after many pores open and close). In many cases, a cascade of short-lived pores is observed on a single vesicle (Fig. 4 and video 1 [28]). The statistical study of the pore duration is shown on Fig. 5(a). It shows that most pores close within 5 s but some of them last over 2 min. We have studied the correlation between the duration of the pore and its rank in a succession of pores on a single vesicle [Fig. 5(b)] and observed that the first pore lasts in general much longer

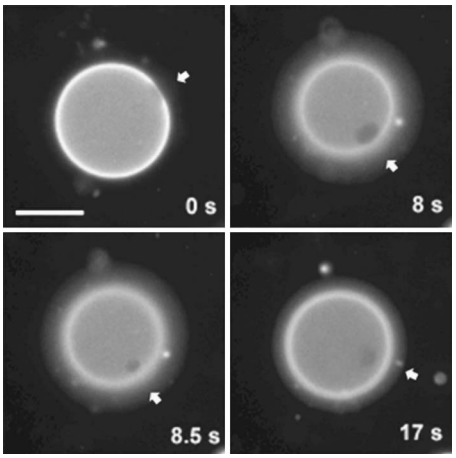

FIG. 4. Cascade of pores on a single vesicle. Each pore (indicated by a white arrow) opens and reseals after less than 2 s. Image 3 shows the closing of the pore of image 2. The bar represents 20 μm.

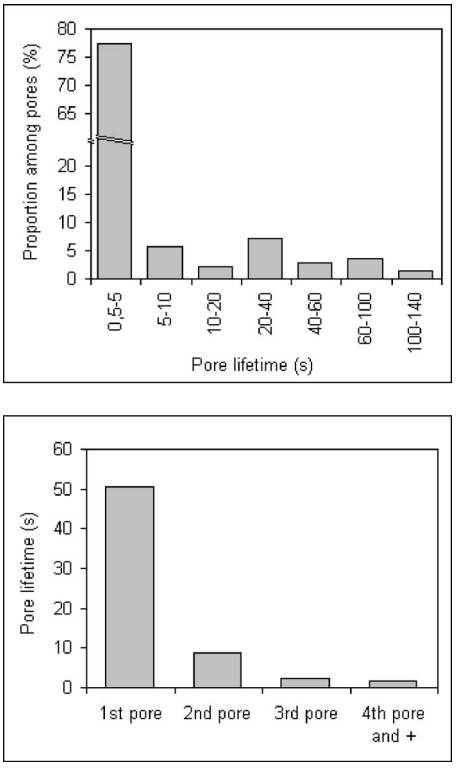

FIG. 5. Statistical studies made over 141 pores. (a) pore duration, (b) correlation between the duration of the pore and its rank in a succession of pores on a single vesicle

(tens of seconds) than the subsequent ones (up to a few seconds).

We have never observed more than one pore at a time on a single vesicle. This is expected because the driving force of the pore formation is the surface tension, and this tension vanishes very quickly after the opening of a large pore.

One advantage of our system (compared to previous experiments into which a pore opens after an illumination of a few tens of minutes or a slow diffusion of detergent) is that we can accurately control the moment when the pore opens and the possible exchange of solution between the vesicle and its outside medium. In our case, the pore opening is simply triggered after a few seconds of illumination. The inner medium of the vesicle is quickly and largely expelled as can be seen from the leaking of small vesicles initially contained inside the main one on Fig. 6 (video 2 [28]). From these pictures (following the exit of a small vesicle), one can infer ν_{leak}, the leaking velocity of the inner medium. For long-lived pores, the closing of the pore is very slow. In this case, Eq. (1) indicates that σ is of the order of ζ/r_{pore}. Thus, from the observed leaking velocity, the line tension can be deduced by modifying Eq. (2) [25],

$$\zeta = \frac{3\pi\eta_{\text{sol}}R_{\text{ves}}}{2}\nu_{\text{leak}}. \tag{12}$$

This is interesting data because it allows inferring ζ from Eq. (12). In Fig. 6 we measure $\nu_{\text{leak}}=8.2\ \mu\text{m/s}$ and deduce $\zeta=1.4$ pN. This value is about ten times lower than the line tension of a membrane edge that would be made of

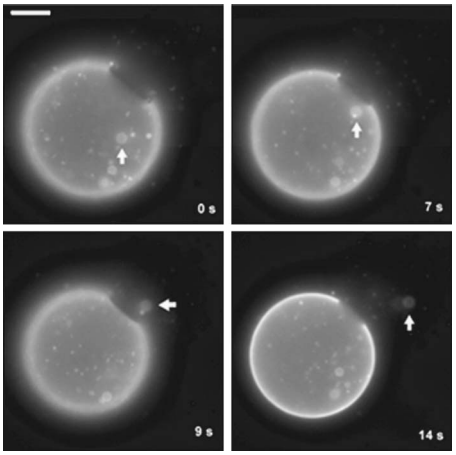

FIG. 6. Leakage of a vesicle during the formation of a long-lived pore. A small vesicle (indicated by a white arrow) is expelled through the pore and allows measuring the leaking velocity. The bar represents 20 μm.

bare DOPC [25]. From 21 experiments, we have measured $\zeta=2\pm1$ pN. It confirms that the C6-NBD-PC or the products of the photosolubilization probably reduce significantly the line tension. A possible explanation is an enrichment of the pore rim in C6-NBD-PC. Figure 7 (video 3 [28]) is another impressive picture showing the leakage of numerous vesicles. It is surprising to see that, in spite of the size and complexity of the inner material, the pore reseals after the leakage.

D. Pore opening and solubilization: Model and numerical simulations

Our hypothesis is that the formation of pores in an aqueous medium can be achieved thanks to the solubilization, which maintains a sufficient surface tension of the vesicle. In order to check this in a quantitative way, it is necessary to postulate the expression of $N(t)$. Since it seems reasonable to think that the solution is self-similar at any time, we can assume that

$$N(t) = N_0 \exp(-t/\tau). \tag{13}$$

$2N_0$ is the initial number of lipids in the vesicle. τ is the solubilization characteristic time, which has to be adjusted to

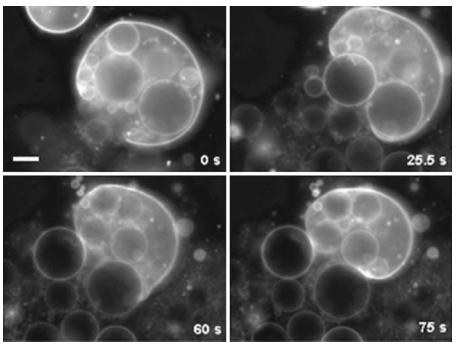

FIG. 7. Leakage of numerous large vesicles inside a bigger one, which finally reseals. The bar represents 20 μm.

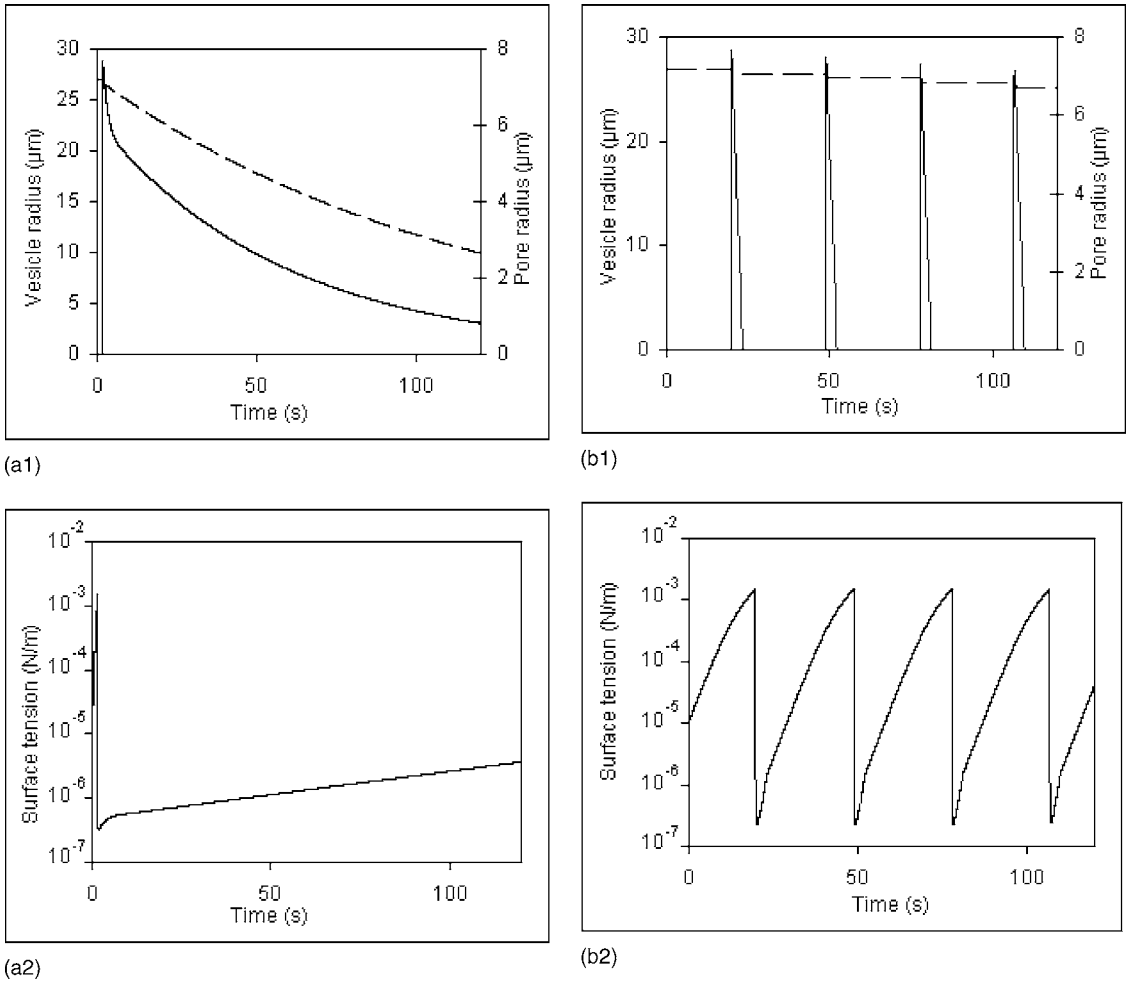

FIG. 8. Simulation of the pore opening and closing. The line tension is set to $\zeta=3$ pN. For all simulations, we decided not to model the energy barrier for the nucleation of a nanometric hydrophilic pore (Ref. [32]) because poorly controlled defects in the membrane can help overcome this barrier (Ref. [25]). For this reason, a minimal pore radius of 2 nm was maintained in the simulations. A pore expands as soon as it reaches a minimum radius $r_{\min}$ obtained for $\sigma=\zeta/r_{\min}$. For $\zeta=1-10$ pN, a nanometric pore expands for $\sigma=0.5-5$ mN/m, which is close to the measured rupture surface tension for DOPC bilayers (Ref. [22]). (a): Strong solubilization regime (characteristic solubilization time $\tau=60$ s). (a1): Evolution of the radius of the vesicle (dotted line) and pore (solid line): a long-lived pore remains open and its size is above optical resolution for 100 s. (a2): Evolution of the surface tension in time: the solubilization causes an increase of the surface tension until it reaches the rupture tension. The tension is then relaxed in few milliseconds when the pore opens and the internal medium leaks out. The leak outflow becomes slow and the solubilization rate is high enough to compete with it and prevents the pore's closing for tens of seconds. (b): Slow solubilization regime (characteristic solubilization time $\tau=800$ s). (b1): Evolution of the radius of the vesicle (dotted line) and pore (solid line): a cascade of short-living transient pores is predicted. (b2): Evolution of the surface tension in time: a new short-lived pore opens as soon as the tension reaches a threshold values close to the rupture surface tension value of a DOPC bilayer.

the leakage rate of the vesicle. With this expression of $N(t)$, Eq. (8) becomes

$$\frac{N_0 \exp(-t/\tau)a_0[1+\sigma(t)/k_s]}{4R_{\text{ves}}^2(t)-r_{\text{pore}}^2(t)} - 1 = \frac{k_BT}{8k_c}\ln\left\{\frac{\pi^2/a_0(1+\sigma/k_s)+\sigma/k_c}{\pi^2/[4R_{\text{ves}}^2(t)-r_{\text{pore}}^2(t)]+\sigma/k_c}\right\}. \quad (14)$$

Figure 8 shows the sequence of pore opening for two solubilization rates obtained by solving the system of Eqs. (1), (4), and (14) with Mathematica. In Fig. 8(a), the solubilization characteristic time τ is set to 60 s and the initial vesicle radius is 27 μm. In that case, a long-lived pore is opened: Its size decreases below optical resolution after more than 100 s. In Fig. 8(b), the characteristic time τ is set to 800 s. In that case, our model predicts a cascade of pores that last less than 5 s and reseal. These results confirm numerically our hypothesis that a sufficient solubilization rate can stabilize a pore opening even in an aqueous medium.

E. Transition from long- to short-living transient pore: Prediction and comparison with experiments

Thus our model predicts that depending on τ, a long-lived pore or a cascade of short-lived pores can be observed. This is confirmed from our experimental data. In the example given in Fig. 2, both regimes are observed successively. For

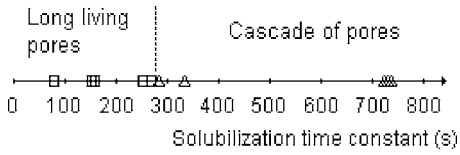

FIG. 9. Correlation between the solubilization rate and the regime of pore that is observed. △ corresponds to experiments in which a cascade of short-lived pores is observed. □ corresponds to experiments in which a single long-lived pore is observed. The position of the symbols on the time axis corresponds to the characteristic solubilization time τ deduced from a decreasing exponential fit of the measured area of the vesicle.

the first 150 s of the experiment, a long-lived pore remains open. Afterwards, we only notice a cascade of transient pores that reseal in less than 5 s. We checked whether the solubilization rates were different during these periods. The solubilization characteristic time constant τ is determined for each period by an exponentially decreasing fit of the vesicle radius. For the first 150 s, the solubilization is fast (τ =215 s); after these 150 s, the solubilization is slower (τ =715 s). This transition from one regime to the other may be explained by the decrease of C6-NBD-PC concentration in the vesicle, which would change τ and therefore switch the vesicle's solubilization regime from one regime to the other.

Other experiments confirm this result. We found that, experimentally, τ could range between 70 and 800 s. This variation may be due to local variation of the amount of C6-NBD-PC, dithionite, or illumination intensity. As previously mentioned, pores can be sorted in two categories according to their lifetime: a cascade of short-lived pores (less than 5 s) or long-lived pores (often a few tens of seconds up to a few minutes). For some vesicles, only one of the regimes was observed. As in the example of Fig. 2, some vesicles successively displayed both regimes. We are able to correlate for each experiment τ and the pore lifetimes (Fig. 9). As it could be intuitively expected, long-lived pores were seen for small τ while short-lived pores were observed with slow solubilization. Experimentally, the value of τ that limits these categories, τ_c, is 275 s for vesicles whose initial radius is close to 20 μm. We propose in the appendix a theoretical estimate of τ_c, the critical solubilization time below which a long-lived pore can be stabilized. An analytical calculation gives some insights about the relevant parameters of the phenomenon and suggests a simple power law,

$$\frac{1}{\tau_c} = \frac{k_B T}{12\pi^2 k_c \eta_{sol}} \frac{\mathrm{s}}{R_{ves}^2}. \tag{15}$$

Our simulation results are well fitted by this law (simulations show that a long-lived pore is predicted for τ values above this analytically computed τ_c while, below τ_c, a cascade of pores is expected). Our observations are well explained too since taking R_{ves}=20 μm (mean size of observed vesicles) and ζ=2 pN, Eq. (15) gives τ_c=307 s, a value that is very close to 275 s, the measured solubilization characteristic time above which no long-lived pores are observed. Equation (15) predicts the possible formation of a long-lived pore and transition from the long-lived pore regime to the cascade of short-lived pores when $R_{\mathrm{ves}}(t)$ decreases. From Eq. (15), a phase diagram predicting the occurrence of a pore lifetime regime can be obtained with the parameters R_{ves}, τ, or ζ. A similar diagram with both regimes of pore lifetime has already been proposed [23] in the case of osmotically stressed vesicles where R_{ves} and the difference of concentration between internal and external media are the parameters.

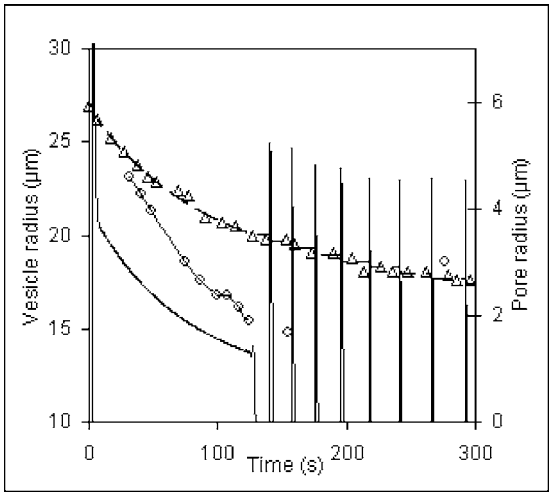

FIG. 10. Comparison between our model's predictions and an experiment. The line tension is set to ζ=3 pN. The best match between the vesicle radius evolution of the vesicle from our experiment and our simulation [Eq. (16)] is obtained for t_1=60 s, t_2 =855 s, p_1=0.41, and p_2=0.59. In that case our simulation predicts the succession of a long-lived pore and a cascade of transient pores. ○: measured pore radius, symbols are linked when they correspond to a single pore that remains open. △: measured vesicle radius. Dotted line: computed vesicle radius. Solid line: computed pore radius.

We have observed some vesicles that displayed both behaviors: a single long-lived pore followed by a cascade of short-lived pores. To obtain a quantitative description of our experiments, a realistic expression of $N(t)$ is needed. This expression must take into account the observed slowing down of the solubilization rate of a vesicle. In order to simulate the transition on a given vesicle, we considered that two solubilization characteristic times, τ_1 and τ_2, could coexist for this vesicle. To validate this assumption, we have fitted our experimental $R_{\mathrm{ves}}(t)$ using the software ORIGIN 6.0 with four free parameters p_1, p_2, τ_1, τ_2,

$$A_p(t) = A_0[p_1 \exp(-t/\tau_1) + p_2 \exp(-t/\tau_2)]. \tag{16}$$

From this fit, we deduce an accurate determination of $N(t)$,

$$N(t) = N_0[p_1 \exp(-t/\tau_1) + p_2 \exp(-t/\tau_2)]. \tag{17}$$

$R_{\mathrm{ves}}(t)$ computed by simulations from Mathematica is thus automatically very close to $R_{\mathrm{ves}}(t)$ measured in our experiments and the actual test for the reliability of our prediction is the accordance between $r_{\mathrm{pore}}(t)$ obtained from experiments and simulations. The results (Fig. 10) are satisfactory since the transition from the long-lived pore to the cascade of pores regimes is accurately predicted. The size (within an accuracy of about 1 μm) and duration of the long-lived pore

are also correctly predicted. These simulations underline the sensitivity of the system; the abrupt switching from the long-lived pore regime to the cascade of pores regime as soon as the solubilization rate becomes too low emphasizes the difficulty to obtain these stabilized long-lived pores in aqueous medium. This decrease of the solubilization rate [Eq. (16)] causes the transition from a long-lived pore to a cascade of short-lived pores and thus explains the correlation between the duration and rank of the pore [Fig. 5(b)].

F. Formation of pores to better understand the membrane solubilization process

Our experiments give interesting clues about the mechanism of membrane solubilization. When more and more detergents are loaded in a membrane, the line tension and the rupture tension of the membrane are lowered because of the conical shape of detergent molecules. These phenomena can lead to rupture of the membrane even if few lipids are extracted from the membrane. The source of the rupture in that case is the cooperative interactions between detergents and their tendency to form a nonlamellar phase. Another possible mechanism is that lipids are extracted from the membrane and the membrane surface tension is raised up; this may be favored by high-detergent concentration and the presence of detergent micelles [10]. According to the relative kinetics of lipid extraction, detergent insertion and subsequent modification of the physical parameters of the membrane, this membrane may open pores before complete fragmentation and surface tension becomes a driving parameter of the solubilization. The kinetics of solubilization may be modified if these pores themselves favor the solubilization process.

IV. CONCLUSION

We found that the combination of C6-NBD-PC, dithionite, and illumination with a mercury lamp induces the stretching of vesicles through the solubilization of the membrane. Our system enables transient pores of micrometric size to open for long periods of time (2 min) in aqueous medium.

We have modified the current model of pore opening and closing to take into account the high surface-tension values and the solubilization of the membrane. The good accordance between our observations and simulations validates these modifications. In addition, this combination of model and experiments has clarified our understanding of the transition between long- and short-lived pores and its relation to the characteristic solubilization time. We are able to reliably deduce interesting physical parameters such as line tension. A potential improvement of the model could take into account the possibility that the edge of the pore is a favorable site for the extraction of lipids from the vesicle and quantify this phenomenon. This could enable us to study the solubilization mechanism (extraction of lipids from the membrane bilayer or from the edges, rupture before loss of material) of various detergents according to their concentrations.

Our system may be suitable to study interactions with edges of membranes, for example with certain proteins [15,29]. The ability to precisely trigger the opening of the pores would be helpful for the control of such experiments. Finally, the system presented here is interesting for the controlled delivery of an encapsulated material. This material can fill most of the high internal space of a giant vesicle as evidenced by Fig. 7 and be released at a perfectly controlled time.

ACKNOWLEDGMENT

The authors thank Tom Melia for careful reading of the manuscript.

APPENDIX: MAXIMUM SOLUBILIZATION TIME FOR A LONG-LIVED PORE

A criterion of pore stability can be inferred from Eq. (1): if a large pore closes slowly, (typically, $-dr_{\mathrm{pore}}/dt < 0.1\ \mu$m/s for a pore of micrometric size that closes during about 1 min), then

$$-\frac{dr_{\mathrm{pore}}}{dt} = -\frac{r_{\mathrm{pore}}}{2\eta_{mb}}\left[\sigma(r_{\mathrm{pore}},N,R_{\mathrm{ves}}) - \frac{\zeta}{r_{\mathrm{pore}}}\right] \approx 0.1\ \mu\mathrm{m/s}. \tag{A1}$$

On the other hand, when a pore remains open, the surface tension is low compared to the rupture tension (or it would entail a very fast leak out). We therefore can use the analytical expression of σ given in Eq. (10),

$$\sigma = \frac{\pi^2 k_c}{a_0}\exp\left[\frac{8\pi k_c(1-Na_0/A_p)}{k_BT}\right].$$

Expressing $A_p = 4\pi R_{\mathrm{ves}}^2 - \pi r_{\mathrm{pore}}^2$, and introducing the parameter $\mathrm{n} = Na_0/4\pi R_{\mathrm{ves}}^2$, we get

$$\sigma(n,r_{\mathrm{pore}},R_{\mathrm{ves}}) = A\exp\left\{B\left[1-n\left(\frac{1}{1-r_{\mathrm{pore}}^2/4R_{\mathrm{ves}}^2}\right)\right]\right\}, \tag{A2}$$

with $A=(\pi^2 k_c)/a_0$ and $B=8\pi k_c/k_BT$. This expression of the tension can be used for the pore radius time derivative, $dr_{\mathrm{pore}}/dt = f(r_{\mathrm{pore}},n,R_{\mathrm{ves}},\zeta)$. As assumed in the text, ζ will be considered constant. For a given value of n, Fig. 11 shows the pore radius derivative as a function of the pore radius. Two cases are possible depending on the value of n. First, when n is below a critical value n_c ($n_c=1.0502$ in the example of Fig. 11 with $\zeta=3$ pN and $R_{\mathrm{ves}}=30\ \mu$m), f equals zero for two r_{pore} values. When n is significantly below n_c only the larger of these values corresponds to a micrometric large pore. Consequently, just after the pore opening the radius of a long-lived pore radius is close to $r_{\mathrm{pore}}^{\max}(n,R_{\mathrm{ves}},\zeta)$, the largest solution of $f(r_{\mathrm{pore}},n,R_{\mathrm{ves}},\zeta)=0\ \mu$m/s. But if n overcomes the critical value n_c then the pore radius derivative remains negative for all r_{pore} and the maximum of f decreases very fast with n: for n very slightly above n_c, the maximum of $f(r_{\mathrm{pore}},n,R_{\mathrm{ves}},\zeta)$ is well below $-0.1\ \mu$m/s and is not compatible with the stability of a long-lived pore. These considerations show that n is a relevant parameter to predict the viability of a long-lived pore.

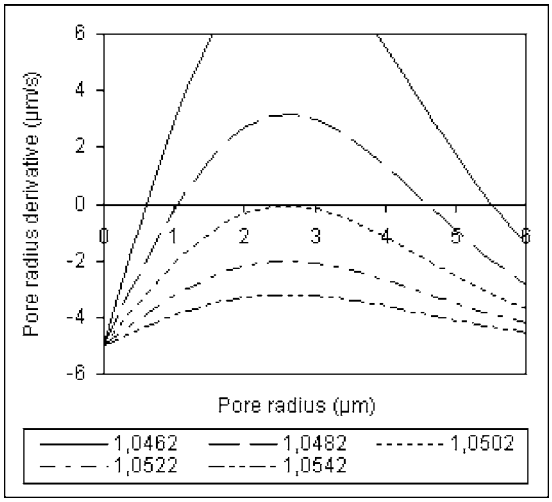

FIG. 11. Force radius time derivative $f^*(r_{\text{pore}},n,R_{\text{ves}},\zeta)$ as a function of r_{pore} for various n with $R_{\text{ves}}=30$ μm and $\zeta=3$ pN. For $n>n_c=1.0502$, $f^*(r_{\text{pore}},n,R_{\text{ves}},\zeta)<-0.1$ μm/s for all r_{pore} and no long-lived pore is expected. For $n<n_c$, $f^*(r_{\text{pore}},n,R_{\text{ves}},\zeta)=-0.1$ μm/s for two r_{pore} values. The larger corresponds to a stable long-lived pore.

We want to derive the expression of τ_c, the solubilization time at the transition between the long-lived pore and the cascade of short-lived pores regimes. We have seen that a long-lived pore is viable as soon as $n=Na_0/4\pi R_{ves}^2$ is less than n_c. It means that the closing of the pore depends on the competition between the solubilization (numerator) and the leakage of the vesicle (denominator). The evolution of $n=N_0\exp(-t/\tau)a_0/4\pi R_{\text{ves}}^2$ is given by its first time derivative, whose sign is that of $-2(dR_{\text{ves}}/dt)-(R_{ves}/\tau)$. $-2(dR_{\text{ves}}/dt)$ is positive while $-(R_{ves}/\tau)$ is negative and remains almost constant during the pore lifetime. Equation (3) gives $dR_{\text{ves}}/dt=-[r_{\text{pore}}^3(t)\sigma(t)]/[6\pi\eta_{\text{sol}}R_{\text{ves}}^3(t)]$. Just after the pore opening, the leakage flow $-4\pi R_{\text{ves}}^2(dR_{\text{ves}}/dt)$ is high and decreases as the pore begins to close. If a long-lived pore regime is reached, the closing is slow and Eq. (1) gives $\sigma\approx\varsigma/r_{\text{pore}}$ so that $-2(dR_{\text{ves}}/dt)\approx r_{\text{pore}}^2\varsigma/3\pi\eta_{\text{sol}}R_{\text{ves}}^3$. According to previous analysis, the long-lived pore regime is possible only if the n derivative reaches zero before n reaches n_c. The most unfavorable case is $-2(dR_{\text{ves}}/dt)-(R_{ves}/\tau)=0$ for $n=n_c$,

$$\frac{1}{\tau}=\frac{r_{\text{pore}}^2(n_c,R_{\text{ves}},\varsigma)\varsigma}{3\pi\eta_{\text{sol}}R_{\text{ves}}^4}. \tag{A3}$$

The pore radius $r_{\text{pore}}^c(R_{\text{ves}},\zeta)=r_{\text{pore}}(n_c,R_{\text{ves}},\zeta)$ and n_c are the solutions of the system,

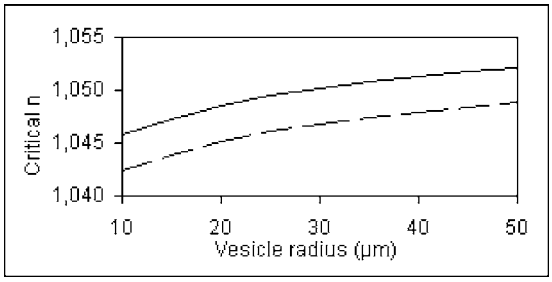

FIG. 12. Critical n_c ($n=Na_0/4\pi R_{\text{ves}}^2$) for $\zeta=3$ pN (solid line) and $\zeta=7$ pN (dotted line).

$$f=\frac{1}{2\eta_{mb}}\left(r_{\text{pore}}A\exp\left\{B\left[1-n\left(\frac{1}{1-r_{\text{pore}}^2/4R_{\text{ves}}^2}\right)\right]\right\}-\varsigma\right)=0, \tag{A4a}$$

$$\frac{\partial f}{\partial r_{\text{pore}}}=\frac{A}{2\eta_{mb}}\exp\left\{B\left[1-n\left(\frac{1}{1-r_{\text{pore}}^2/4R_{\text{ves}}^2}\right)\right]\right\}\times\left[1-\frac{r_{\text{pore}}^2}{2R_{\text{ves}}^2(1-r_{\text{pore}}^2/4R_{\text{ves}}^2)^2}Bn\right]=0. \tag{A4b}$$

Even though this system can be solved numerically (results are shown on Fig. 12), an analytical resolution can also be obtained given that $n\sim 1$ and $r_{\text{pore}}\ll R_{\text{ves}}$. A first-order development of Eq. (A4b) gives

$$r_{\text{pore}}^c\approx\sqrt{\frac{2}{Bn}}R_{\text{ves}}\approx\sqrt{\frac{k_BT}{4\pi k_c}}R_{\text{ves}}, \tag{A5a}$$

which implies from Eq. (A4a),

$$n_c\approx 1-\frac{k_BT}{8\pi k_c}\ln\left(\frac{2\varsigma a_0}{\pi^{3/2}R_{\text{ves}}\sqrt{k_ck_BT}}\right). \tag{A5b}$$

From this computation, we can deduce from Eq. (A3) the maximum value of τ above which no long-lived pore can be expected,

$$\frac{1}{\tau_c}\approx\frac{k_BT\varsigma}{12\pi^2k_c\eta_{\text{sol}}R_{\text{ves}}^2}. \tag{A6}$$

This simple power law is in very good agreement with our simulation results (simulations show that cascade of pores are predicted for τ values above this computed τ_c and a long-lived pore is predicted either).

[1] E. H. Moase, W. Qi, T. Ishida *et al.*, Biochim. Biophys. Acta **1510**, 43 (2001).
[2] J. A. Zasadzinski, Curr. Opin. Solid State Mater. Sci. **2**, 345 (1997).
[3] T. M. Allen, C. B. Hansen, and D. E. Lopes de Menezes, Adv. Drug Delivery Rev. **16**, 267 (1995).
[4] M. S. Spector, J. A. Zasadzinski, and M. B. Sankaram, Langmuir **12**, 4704 (1996).
[5] U. Kragh-Hansen, M. le Maire, and J. V. Moller, Biophys. J. **75**, 2932 (1998).
[6] M. le Maire, P. Champeil, and J. V. Moller, Biochim. Biophys. Acta **1508**, 86 (2000).
[7] M. Ollivon, S. Lesieur, C. Grabielle-Madelmont *et al.*, Biochim. Biophys. Acta **1508**, 34 (2000).

[8] A. M. Seddon, P. Curnow, and P. J. Booth, Biochim. Biophys. Acta **1666**, 105 (2004).
[9] K. Edwards and M. Almgren, J. Colloid Interface Sci. **147**, 1 (1991).
[10] M. Almgren, Biochim. Biophys. Acta **1508**, 146 (2000).
[11] J. Knol, K. Sjollema, and B. Poolman, Biochemistry **37**, 16410 (1998).
[12] K. A. Riske and R. Dimova, Biophys. J. **88**, 1143 (2005).
[13] E. Tekle, R. D. Astumian, W. A. Friauf *et al.*, Biophys. J. **81**, 960 (2001).
[14] J.-C. Bradley, M.-A. Guedeau-Boudeville, G. Jandeau *et al.*, Langmuir **13**, 2457 (1997).
[15] A. Saitoh, K. Takiguchi, Y. Tanaka *et al.*, Proc. Natl. Acad. Sci. U.S.A. **95**, 1026 (1998).
[16] O. Sandre, L. Moreaux, and F. Brochard-Wyart, Proc. Natl. Acad. Sci. U.S.A. **96**, 10591 (1999).
[17] F. Nomura, M. Nagata, T. Inaba *et al.*, Proc. Natl. Acad. Sci. U.S.A. **98**, 2340 (2001).
[18] F. Brochard-Wyart, P. G. de Gennes, and O. Sandre, Physica A **278**, 32 (2000).
[19] M. Colleau, P. Hervé, P. Fellmann *et al.*, Chem. Phys. Lipids **57**, 29 (1991).
[20] M. I. Angelova, S. Soléau, P. Méléard *et al.*, Prog. Colloid Polym. Sci. **89**, 127 (1992).
[21] L. Mathivet, S. Cribier, and P. F. Devaux, Biophys. J. **70**, 1112 (1996).
[22] W. Rawicz, K. C. Olbrich, T. McIntosh *et al.*, Biophys. J. **79**, 328 (2000).
[23] M. A. Idiart and Y. Levin, Phys. Rev. E **69**, 061922 (2004).
[24] W. Helfrich and R.-M. Servuss, Nuovo Cimento Soc. Ital. Fis., D **3**, 137 (1984).
[25] E. Karatekin, O. Sandre, H. Guitouni *et al.*, Biophys. J. **84**, 1734 (2003).
[26] R. Bar-Ziv, E. Moses, and P. Nelson, Biophys. J. **75**, 294 (1998).
[27] N. Rodriguez, J. Heuvingh, F. Pincet *et al.*, Biochim. Biophys. Acta **1724**, 281 (2005).
[28] See EPAPS Document No. E-PLEEE8-74-016611 for visualizing corresponding videos. For more information on EPAPS, see http://www.aip.org/pubservs/epaps.html.
[29] I. V. Polozov, G. M. Anantharamaiah, J. P. Segrest *et al.*, Biophys. J. **81**, 949 (2001).
[30] Z. Chen and R. P. Rand, Biophys. J. **73**, 267 (1997).
[31] S. Tristram-Nagle, H. I. Petrache, and J. F. Nagle, Biophys. J. **75**, 917 (1998).
[32] R. W. Glaser, S. L. Leikin, L. V. Chernomordik *et al.*, Biochim. Biophys. Acta **940**, 275 (1988).